

# Evaluation of the impacts of tunnelling on the hydrogeological environment under a coastal urban site, Korea

HYOUNG SOO KIM<sup>1</sup>, WOON SANG YOON<sup>2</sup>, JIN MOO LEE<sup>3</sup> &  
SANG WOO WOO<sup>4</sup>

<sup>1</sup> Nexgeo ltd. (e-mail: hskim@nexgeo.com)

<sup>2</sup> Nexgeo ltd. (e-mail: gaia@nexgeo.com)

<sup>3</sup> SK engineering & construction.

<sup>4</sup> SK engineering & construction. (e-mail: swwoo-a@skec.co.kr)

**Abstract:** Tunnelling often destroys and changes the hydro-geological environment abruptly, usually in a specific section of the works. When tunnelling under an urban site, various hydro-geohazards such as drying up and subsidence can be initiated. This paper concerns the construction of a section of about 6km of the Korea Train Express at an average depth of 50m and located 1km from the coast at Busan, Korea. The site is an area of foreshore reclamation that has been developed periodically since the late 1800s; two underground lines have been constructed between 1981~1994 and 1994~2001 respectively. This paper concerns an evaluation into the change of groundwater flow and seawater intrusion, as it was highly possible that the tunnelling would cause drawdown of the water table and salt damage in the project site. Various field tests have been executed to determine the hydro-geological properties of the aquifers including four representative parameters, i.e., transmissivity, storativity, longitudinal dispersivity, and effective porosity. The likely change of groundwater flow by the effect of tunnelling was analysed initially. The simulated numerical results predicted a maximum drawdown of 17.2m with total inflow into the tunnel in the range from 0.33 to 2.52ton/min/km. Based on the above results, the seawater intrusion by tunnelling was simulated using a three dimensional numerical model which considered density dependant fluid flow. The results indicated that seawater might intrude toward the tunnelling region in the range of 200~220m from the initial interface between seawater and groundwater.

**Résumé:** Perçage d'un tunnel fait souvent des destructions et des changements abrupts, habituellement dans un secteur spécifique des travaux. En perçant un tunnel sous l'emplacement urbain, il pourrait se produire des divers risques hydrogéologiques, tel que épuisement de l'eau, l'affaissement, etc. Dans ce projet de la construction du Korea Train Express qui est environ 6km à la longueur, 50m à la profondeur moyenne sous la terre, et 1km localisé de la côte du Busan, Corée du Sud. En ce qui concerne l'emplacement, on a recouvert des lais périodiquement à partir de la fin des années 1800, et où l'on a déjà construit deux lignes de métro, l'un en 1981~1994 et l'autre en 1994~2001. On a exécuté des évaluations sur les changements des courants d'eaux souterraines et l'intrusion d'eau salée, car il est bien possible que perçage d'un tunnel causerait l'abaissement des couches d'eau souterraine ou des dommages par l'eau salée. De divers études sur le terrain ont été exécutés sur les propriétés hydrogéologiques de ces couches aquifères incluant quatre paramètres représentatifs, c.-à-d., transmissivité spécifique, contenance, longitudinal dispersivity, et porosité. D'abord, Nous avons analysé la simulation numérique sur le changement de l'écoulement d'eaux souterraines par l'effet du perçage d'un tunnel. Les résultats numériques ont montré que l'abaissement maximum du niveau était 17.2m et l'apport total de l'eau dans le tunnel avait la gamme de 0,33 à 2.52ton/min/km. Basé sur les résultats ci-dessus, l'intrusion de l'eau salée par le perçage d'un tunnel a été simulée avec le modèle numérique tridimensionnel qui a considéré le flux fluide dépendant de la densité. Les résultats ont montré que l'eau salée s'avancé vers la région de perçage d'un tunnel dans les gammes de 200~220m de l'interface initiale de l'eau salée et les eaux souterraines.

**Keywords:** tunnels, excavation, geological hazards, hydrogeology, numerical model

## INTRODUCTION

Accurate evaluation and prediction of the impact of tunnelling on hydrogeologic environments is one of the most important assessments in planning the construction of tunnels in urban areas in order to minimise impact on the existing facilities. In this case, close to the coast, it was necessary to predict seawater intrusion as well as the change of groundwater flow system.

The Kumjung tunnel is to be the longest tunnel constructed along the Seoul-Busan high speed railway of Korea. The tunnel consists of two lots, 14-2 and 14-3, which form a part of the railway between 393km and 409km away from the starting point in Seoul. The total length of the Kumjung tunnel is 18.6km, 12.9km of which is to be constructed through the Kumjung Mountain and 5.7km through the central urban area of Busan. The estimated construction period of the Kumjung tunnel is approximately 54 months. Standard support patterns were envisaged for two partial sections of the tunnel, one through hard rock with enlargement after TBM excavation and the other, intersecting the Dongrae fault, using mechanical excavation. This paper concerns the latter. In detail, our study site, the construction on the line of Korea Train Express, is about 5.7km in length, 50m in average depth under the ground, and located on a site separated about 1km from the coast in Busan, Korea as shown in Figure 1. The purpose of this paper is to evaluate and predict impact of the seawater intrusion by the investigation, tests, and numerical models

systematically based on groundwater flow and density dependant transport. As the result, we were able to propose prevention and control of seawater on this construction works.

## FIELD STUDY

### Geologic condition

The geology of the Kumjung tunnel consists of Cretaceous volcanic rock intruded by gabbro, granodiorite and biotite granite. A partial section of lot 14-3 near the endpoint is dominated by alluvium which is mainly composed of silty sand or clay. The geological map of lot 14-3 is shown in Figure 1. The Dongrae fault is a large scale strike-slip fault which runs N20-30E and is tens of kilometres in length. Major design consideration needed to be given to the fault because it intersects the tunnel route near the endpoint, forming a weak zone of weathered and fractured rock.

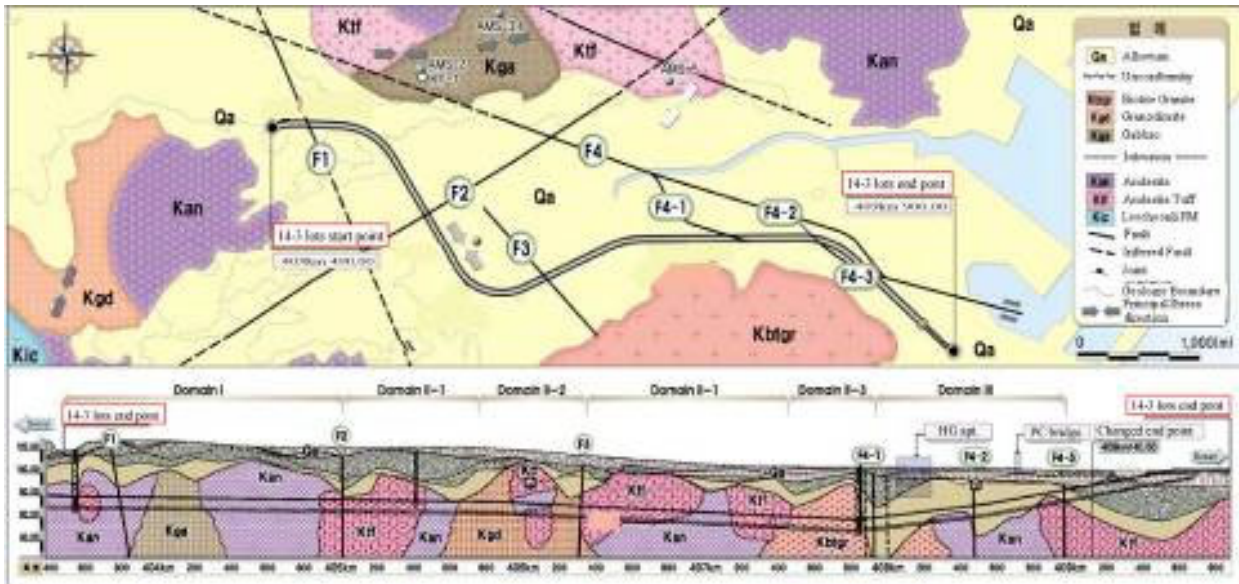


Figure 1. Engineering geotechnical map on the study area

### Hydrogeologic condition

Various groundwater field tests were carried out to evaluate the hydraulic properties of this study area as shown in Table 1.

Table 1. The purpose and number of groundwater field tests

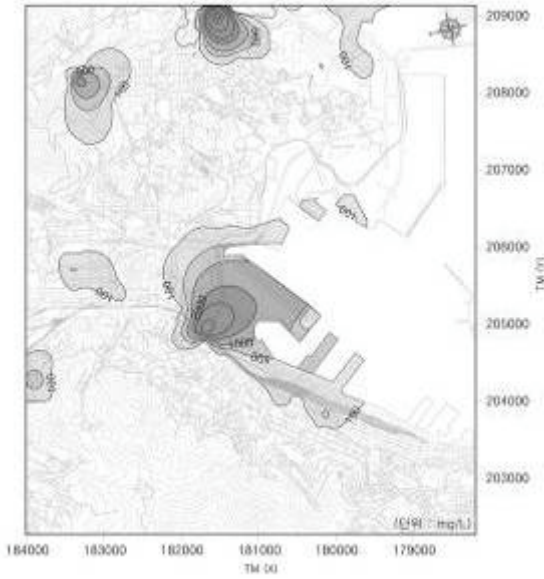
	Packer test	Slug test	Pumping test	Flowing fluid logging test	Tracer test	Water quality analyses
Transmissivity	O	O	O	O		
Storativity		O	O			
Longitudinal dispersivity					O	
Effective porosity					O	
Number of test	125	10	5	5	2	1296

One hundred and twenty five packer tests in forty four boreholes were conducted in the fractured zone of rock. Ten slug tests in several boreholes which had very well weathered fractured zones were performed instead of standard packer tests. For reliability and calibration of packer and slug test results, five 24-hour pumping tests and flowing fluid logging tests were added. The tested volume of aquifer for pumping test are greater that that for other tests. Packer and slug test results required up scaling by factors of 1.4 ~ 3.2 to match pumping test results. Similar scale effects were reported in numerous other study sites (Nastev et al. 2004). The flowing fluid logging tests can be analyzed to identify depth locations of inflow and evaluate the transmissivity and salinity of the fluid at each inflow point. This test is similar to packer test in point view of obtaining the hydraulic conductivity in each test interval but able to measure in-flow as well as out-flow through discontinuities in the rock in detail. The hydraulic conductivity resulted from various tests ranges from  $9.58 \times 10^{-5} \sim 7.55 \times 10^{-6} \text{ m/s}$ . We have performed the tracer test and water quality (EC, salinity, pH, Temperature, TDS) analyses related with solute transport for evaluation on seawater intrusion as shown in Table 1. Two natural gradient tracer tests were performed and we had the values of longitudinal dispersivity having ranges from 0.5 to 5.5 and effective porosity having those from 0.05 to 0.21 as shown in Table 2. One thousand two hundred and ninety six water quality analyses were measured for the degree of seawater intrusion and

the boundary between groundwater and seawater under this study area. Figure 2 shows the distribution of concentration of chloride ion and may be able to assume the interface between seawater and groundwater in this study area. This result was used to identify the initial boundary condition of the interface between groundwater and seawater. These results were divided into four engineering formations .i.e., weathered soil, weathered rock, fractured rock, and hard rock as shown in Table 2.

**Table 2.** Representative hydraulic properties of each material type from groundwater field tests

Type	groundwater flow			contaminant transport	
	$K(\text{cm/sec})$	$S$		$n_e$	$\alpha_t(m)$
		$S_s(m^{-1})$	$S_y$		
weathered soil	$9.58 \times 10^{-5}$	$3.4 \times 10^{-3}$	0.20	0.21	5.5
weathered rock	$1.74 \times 10^{-5}$	$2.3 \times 10^{-3}$	0.12	0.15	4.2
fractured rock	$9.73 \times 10^{-6}$	$1.3 \times 10^{-4}$	0.09	0.08	3.3
hard rock	$7.55 \times 10^{-6}$	$6.9 \times 10^{-5}$	0.05	0.05	0.5



$$\theta \frac{\partial C}{\partial t} + \rho_b \frac{\partial S}{\partial t} + V \cdot \nabla C - \nabla \cdot (\theta D \cdot \nabla C) = \left[ \left( \alpha \rho_o g \frac{\theta}{n_e} + \beta \rho_o g \theta + n_e \frac{d\theta}{dh} \right) \frac{\partial h}{\partial t} + \frac{\rho}{\rho_o} V \cdot \nabla \left( \frac{\rho}{\rho_o} \right) - \frac{\partial \theta}{\partial t} \right] C \quad (2)$$

where,  $\rho_b$  is the bulk density of the medium,  $C$  is the material concentration in aqueous phase,  $S$  is the material concentration in adsorbed phase,  $C_m$  is the concentration of the injection fluid,  $t$  is the time,  $D$  is the dispersion coefficient tensor,  $\lambda$  is the decay constant,  $m$  is the external source/sink,  $K_w$  is the first-order biodegradation rate constant through dissolved phase, and  $K_s$  is the first order biodegradation rate constant through adsorbed phase.

## Groundwater flow

### Model description and result

The distribution of groundwater under urban sites can be complex and quite different to that under undeveloped mountainous terrain. This distribution may result from disturbance by previous subway lines, buildings, apartments, factories and so on. Figure 3 shows the distribution of water table as measured in 54 boreholes in the study area and indicates the common properties of urban sites. The commercial program, Visual MODFLOW v3.0, was used to simulate the changes of hydrogeologic condition induced by tunnelling. This programme is a three dimensional finite difference modeling using variable boundary condition for saturated porous media (McDonald & Harbaugh, 1988). A finite element mesh used in simulations was composed of a total of 688,080 nodes (188x305x12). The size of the whole domain is 7240m, 4020m, and 400m in x (north - south), y (east - west), and z direction, respectively. The advance rate of excavation was assumed to be 4m/day for the transient state condition.

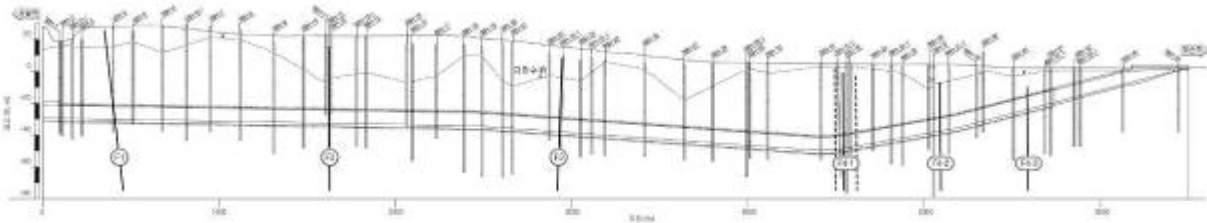


**Figure 3.** Distribution of water table as measured by 54 boreholes in the study area

Maximum drawdown was predicted to be 17.2m and the radius of influence about 120m in the study area. Total inflows into the tunnel were simulated in the range from 0.33 to 2.52ton/min/km. The simulated numerical results showed that groundwater flowed toward the drain boundary condition which described the excavation by tunnelling in the spatial distribution of total head and Darcy velocity field as shown in Figure 4 before tunnelling and Figure 5 after tunnelling.

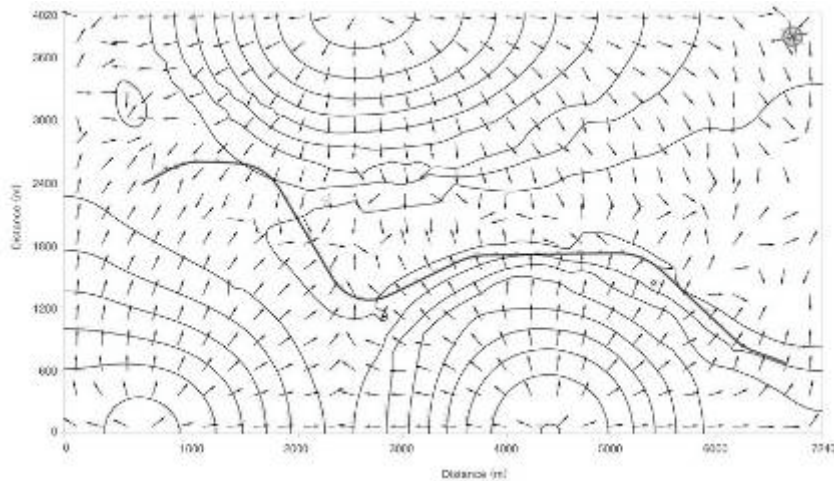


**Figure 4.** The spatial distribution of total head and Darcy velocity field before tunnelling

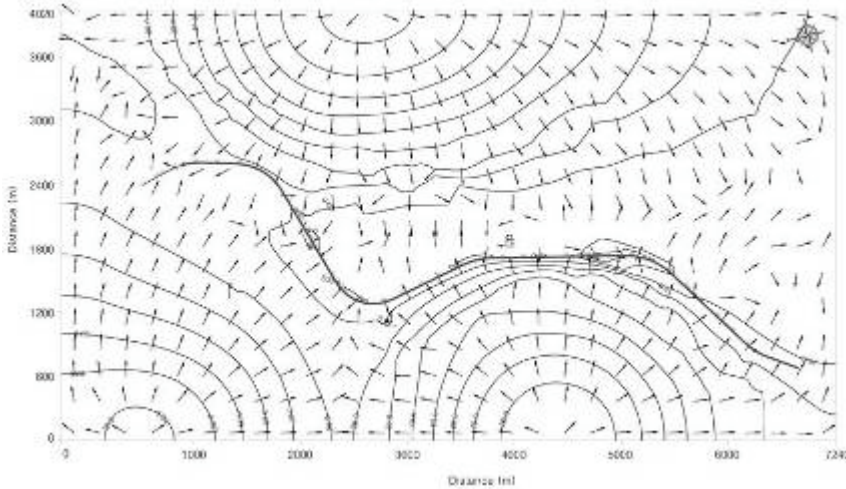


Figure 5. The spatial distribution of total head and Darcy velocity field after tunnelling

## Seawater intrusion

### Model description

This study area is about 1km from the coast in Busan, Korea. The site has been periodically reclaimed since the late 1800s. It is very important to determine the initial interface between seawater and groundwater for prediction by numerical simulation of seawater intrusion. As stated above, we have assumed the interface from the results of the water quality analyses and put this into the numerical simulation as a boundary condition between seawater and groundwater. Also, the above numerical simulation results on groundwater flow were used as the initial condition. The density dependent flow must be considered as well as solute transport on evaluation of seawater intrusion and we have used the FEFLOW v5.1, the commercial program which is a three dimensional finite element groundwater flow and transport model for variable saturated porous media (Diersch, 2004). The node points and elements used in this model were 17,402 and 29,256 respectively. This model size is similar to with the earlier model on groundwater flow. We divided the model into five layers with hydraulic properties of flow and transport data as shown in Table 3.

Table 3. The hydraulic properties of flow and transport data

	layer		Hydraulic conductivity ( $K$ , cm/sec)	Storativity ( $S_s$ , $m^{-1}$ )	Infiltration (mm/year)	Density rate ( $10^{-4}$ )
	no.	Dep.(m)				
flow data	1		$1.08 \times 10^{-4}$	$4.8 \times 10^{-3}$	83	250
	2	-10	$1.74 \times 10^{-5}$	$2.3 \times 10^{-3}$	-	250
	3	-20	$9.73 \times 10^{-6}$	$1.3 \times 10^{-4}$	-	250
	4	-30	$7.55 \times 10^{-6}$	$6.9 \times 10^{-5}$	-	250
	5	-50	$7.55 \times 10^{-6}$	$6.9 \times 10^{-5}$	-	250
	layer		Effective porosity( $n_e$ )	Diffusion coefficient ( $10^9 m^2 s^{-1}$ )	Longitudinal dispersivity (m)	Transverse dispersivity (m)
	no.	Dep.(m)				
transport data	1		0.21	$3.565 \times 10^3$	20	2
	2	-10	0.15	$3.565 \times 10^3$	5.5	2.3
	3	-20	0.11	$3.565 \times 10^3$	4.2	0.9
	4	-30	0.09	$3.565 \times 10^3$	3.3	0.8
	5	-50	0.05	$3.565 \times 10^3$	0.5	0.05

Firstly, we attempted to simulate seawater intrusion due to the previously excavated subway lines. Two possible interfaces between seawater and groundwater were used as initial boundary conditions. Firstly, we used the present coast line as a boundary condition (a minimal assumption). Secondly, we used the measured field data for maximum impact. The two simulation results showed no difference for the interfaces between seawater and groundwater because of the small radius of influence of the subway lines. Based on the above simulated results, the seawater intrusion by tunnelling was simulated as transient state condition for the effect of tunnel advance rate. The simulations indicated a longitudinal seawater intrusion of the order of 200 to 220m toward the tunnelling region from the interface as shown in Figure 6 and 7. The seawater intrusion occurred mainly in the period up to 400 days after tunnelling after which there was an additional 10~20m for 1500 days. So we estimated re-balance of the interface between seawater and groundwater after 1500 days by the simulated result.

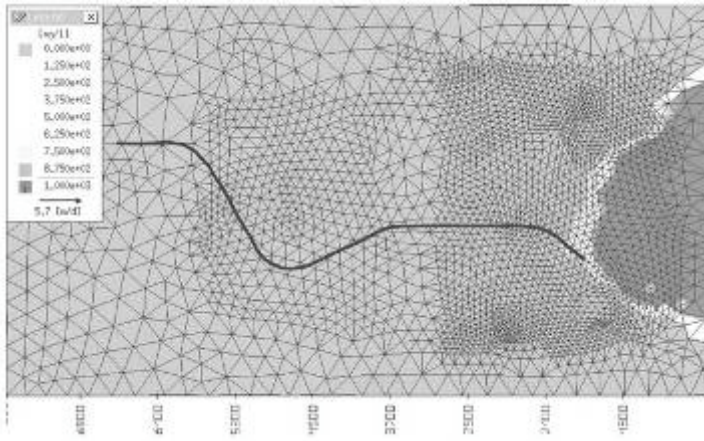


Figure 6. The spatial distribution of seawater intrusion before tunnelling

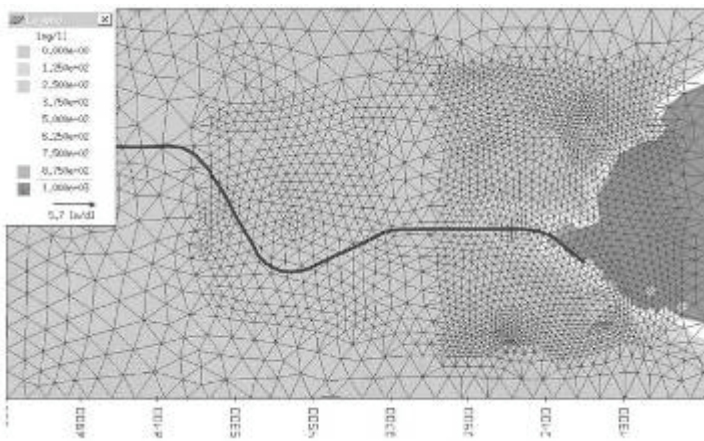


Figure 7. The spatial distribution of seawater intrusion by impact of tunnelling

## CONCLUSIONS

This study initially involved simulating changes in groundwater flow induced by tunnelling. The simulated numerical results showed a maximum drawdown was 17.2m and a total inflow into the tunnel of between 0.33 and 2.52ton/min/km. This simulated result may overestimate the impact of tunnelling rather than real conditions because of assuming the worst case. However, it is very necessary to evaluate urban groundwater environmental systems for minimizing potential geo-hazards especially as the study site had very complex groundwater environmental system as indicated by the field investigation. Following the above results, the seawater intrusion by tunnelling was simulated using a three dimensional numerical model which allowed for density dependant fluid flow. The results showed the seawater intruded toward the tunnelling region in the range of 200~220m from the initial interface between seawater and groundwater. The amount of seawater intrusion is limited for much of the tunnelling because the general (normal) groundwater flow is towards the sea. In some areas systems for preventing seawater intrusion might be needed at an early stage of the construction because of the high possibility of seawater intrusion. In addition to prediction by numerical simulation, four wells were installed at sites with a relatively high possibility of seawater-intrusion for close monitoring of water table levels and water qualities (EC, TDS, salinity, pH) and temperature.

**Acknowledgements:** The work presented in this paper was carried out with funding from SKEC (SK engineering & construction).

**Corresponding author:** Mr Hyung Soo Kim, NexGeo Ltd., 134-1, Garak2-Dong, Songpa-Gu, Seoul, 138-807, South Korea. Tel: +82 2 448 6953. Email: hskim@nexgeo.com.

## REFERENCES

CHENG, H.P., G.T. YEH, J. XU, M.H. LI, & R. CARSEL. 1998. A study of incorporation the multigrid method into the three-dimensional finite element discretization: A modular setting and application. *International Journal of Numerical Methods for Engineering*, **41**, 499-526.

- CHIN- FU TSANG & CHRISTINE DOUGHTY. 2003. Multirate flowing fluid electric conductivity logging method. *Water Resources Research*, **39**(12), 1354 – 1363.
- DIERSCH, H.J.G. 2004. *FEFLOW v5.1*, WASY Institute for Water Resources Planning and Systems Research Ltd., Berlin, Germany.
- GALEATI, G., G. GAMBOLATI, & S. P. NEUMAN. 1992. Coupled and partially coupled Eulerian-Lagrangian model of freshwater-seawater mixing. , *Water Resources Research*, **28**(1), 149-165.
- MCDORALD, M.G., AND A.W. HARBAUGH. 1988. *A modular three-dimensional finite difference ground-water flow model*. Techniques of Water-Resources Investigations, U.S.G.S.
- NASTEV M., M.M. SAVARD, P. LAPCEVIC, R.LEFEBRVE, & R. MARTEL. 2004. Hydraulic properties and scale effects investigation in regional rock aquifer, south-western Quebec, Canada. *Hydrogeology Journal*, **12**(3), 257 - 269.
- YEH, G.T. 1999. *Computational subsurface hydrology*. Kluwer academic publishers, 277pp.
- YOUNG, S.C., H.E. JULIAN, H.S. PEARSON, F.J. MOLZ, & G.K. BOMAN. 1998. *Application of the electromagnetic borehole flowmeter*, EPA/600/R-98/058. U.S. Environmental Protection Agency.